New Structural Motifs in Metallaborane Chemistry. Synthesis, Characterization, and Solid-State Structures of $(Cp^*W)_3(\mu\text{-}H)B_8H_8$, $(Cp^*W)_2B_7H_9$, and $(Cp^*Re)_2B_7H_7$ ($Cp^* = \eta\text{-}C_5Me_5$)

Andrew S. Weller, Mayou Shang, and Thomas P. Fehlner*

Department of Chemistry and Biochemistry, University of Notre Dame, Notre Dame, Indiana 45665

Received September 29, 1998

Hydrogen loss from the 7 skeletal electron pair (sep) nido 2-$Cp^*H_3WB_4H_8$, **1** ($Cp^* = \eta\text{-}C_5Me_5$), the metal analogue of pentaborane (**9**), has been examined as a potential source of unsaturated, reactive species. Pyrolysis of **1** leads to 6 skeletal electron pair $(Cp^*W)_2B_5H_9$, **2** (45%), 7 sep $Cp^*{}_3W_3(\mu\text{-}H)B_8H_8$ **3** (19%), and 7 sep $(Cp^*W)_2B_7H_9$, **4** (low yield), whereas photolysis gives **2** (52%) and **4** (7%). Compound **2** is known, and **3** and **4** have been spectroscopically and crystallographically characterized. Further, the isoelectronic and nearly isostructural analogue of **4**, $(Cp^*Re)_2B_7H_7$, **5**, has been prepared from the reaction of Cp^*ReCl_4 and BH_3·THF in 66% yield. It is demonstrated that **3** exhibits a skeletal structure corresponding to a highly capped W_3 bonded triangle and is analogous to a known multinuclear Ru_{11} cluster with a hexagonal close packed metal core. As such it constitutes an example of a closed, boron-rich metallaborane cluster with ($n - 4$) sep. Likewise, it is shown that **4** and **5** possess unusual structures and constitute examples of closed metallaborane clusters with ($n - 2$) sep. Fenske−Hall MO calculations show that the observed cluster shapes are appropriate for the observed sep's. These two new cluster types demonstrate that transition metal fragments can be used to manipulate the cluster bonding network of a borane, effectively collapsing a single cage into a more closely packed network.

Introduction

The rationalization of the structural patterns exhibited by boranes by Williams[1] and the development of empirical electron counting rules by Wade[2] and Mingos[3] gave us the paradigm for rationalizing structure in cluster chemistry. Concurrently, the isolobal analogy,[4,5] which allows transition metal and main group fragments to be mapped onto one another on the basis of frontier orbital energies and occupancies, facilitated the development of metallaborane chemistry. These ideas allow not only the rationalization of cluster shapes in which a transition metal fragment subrogates a {BH} group but also the conceptual design of new metallaboranes.

We have recently been exploring the reactivity of {Cp*M} fragments with the monoboron reagents BH_3·THF and $LiBH_4$. For later transition metals, e.g., Co,[6] Rh,[7] and Ru,[8] which contribute two, two, and one electrons, respectively, to cluster bonding, the structures that result fit nicely into the established motifs for borane clusters. Earlier transition metal fragments such as {Cp*Cr},[9] {Cp*Mo}[10] and $\{Cp^*TaCl_2\}$,[11] have formal frontier orbital populations considerably less than 2. Relative to {BH}, and metal fragments analogous to {BH}, these fragments are electronically unsaturated and their presence in a metallaborane can generate unexpected behavior.[12]

An interesting question arises as to what the structural response would be if more boron vertexes were added, while keeping the metals formally unsaturated with respect to cluster bonding. In transition metal clusters low formal electron counts lead to highly capped cluster structures which often resemble small fragments of close packed metals.[5] For example, $[Os_{10}H_4(CO)_{24}]^{2-}$ [13] may be described as a tetracapped octahedron associated with 134 cluster valence electrons (cve) or 7 skeletal electron pairs or, on the other hand, as a condensed, cubic close packed metal fragment encapsulated in ligands.[5] However, such behavior has not been observed in borane or metallaborane clusters.

(1) Williams, R. E. *Adv. Inorg. Chem. Radiochem.* **1976**, *18*, 67.
(2) Wade, K. *Adv. Inorg. Chem. Radiochem.* **1976**, *18*, 1.
(3) Mingos, D. M. P.; Johnston, R. L. *Struct. Bonding* **1987**, *68*, 29.
(4) Hoffmann, R. *Angew. Chem., Int. Ed. Engl.* **1982**, *21*, 711.
(5) Mingos, D. M. P.; Wales, D. J. *Introduction to Cluster Chemistry*; Prentice Hall: New York, 1990.
(6) Nishihara, Y.; Deck, K. J.; Shang, M.; Fehlner, T. P.; Haggerty, B. S.; Rheingold, A. L. *Organometallics* **1994**, *13*, 4510.
(7) Lei, X.; Shang, M.; Fehlner, T. P. *J. Am. Chem. Soc.* **1998**, *120*, 2686.
(8) Lei, X.; Shang, M.; Fehlner, T. P. *Inorg. Chem.* **1998**, *37*, 3900.
(9) Ho, J.; Deck, K. J.; Nishihara, Y.; Shang, M.; Fehlner, T. P. *J. Am. Chem. Soc.* **1995**, *117*, 10292.
(10) Aldridge, S.; Shang, M.; Fehlner, T. P. *J. Am. Chem. Soc.* **1998**, *120*, 2586.
(11) Aldridge, S.; Hashimoto, H.; Shang, M.; Fehlner, T. P. *Chem. Commun.* **1998**, 207.
(12) Fehlner, T. P. *J. Chem. Soc., Dalton Trans.* **1998**, 1525.
(13) Braga, D.; Henrick, K.; Johnson, B. F. G.; Lewis, J.; McPartlin, M.; Nelson, W. J. H.; Sironi, A.; Vargas, M. D. *Chem. Commun.* **1983**, 1131.

10.1021/om980814c CCC: $18.00
Publication on Web 02/05/1999

Chart 1

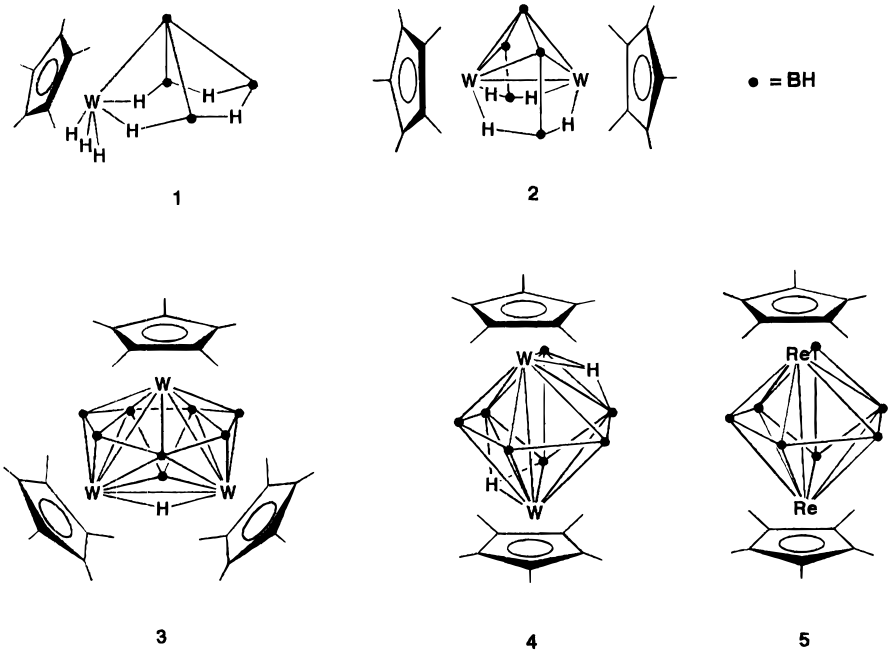

We have previously reported the preparation and isolation of useful quantities of the monotungstaborane *nido*-2-$(Cp^*WH_3)B_4H_8$, **1** (Chart 1),[14] and now have examined its reactivity.[15] Although compound **1** is a metallaborane, an analogue of pentaborane (**9**), it bears three hydride ligands. Further, it is generated from $Cp^*WCl_4 + 4BH_4^-$ via facile H_2 elimination. Additional H_2 elimination would generate a 16-electron metal center, and the consequent chemistry should reflect the effects of a {Cp*W} fragment on cluster bonding.

In fact, the reactivity of organometallic cyclopentadienyl hydrides of the type $(\eta^5\text{-}C_5R_5)_2MH_n$ (R = H, Me; M = Ta; n = 3; M = W n = 2) is well documented.[16,17] Thermal or photolytic conditions are commonly used to activate the metal center, resulting in reductive elimination of H_2. For example Bercaw has shown that thermolysis of $Cp^*_2TaH_3$ in the presence of CO affords the monohydride Cp^*_2TaHCO,[18] while Green[19] and others,[20] have demonstrated that the photolytic activation of $(\eta^5\text{-}C_5R_5)_2WH_2$ (R = H, Me) affords the reactive 16-electron intermediate $(\eta^5\text{-}C_5R_5)_2W$ (R = H, Me), which is capable of inserting into C−H bonds. Thus, we have investigated the thermolytic and photolytic chemistry of **1** giving $(Cp^*W)_3(\mu\text{-}H)B_8H_8$, **3**, and $(Cp^*W)_2B_7H_9$, **4**, as new compounds.[21] We also describe the synthesis of the dirhenaborane $(Cp^*Re)_2B_7H_7$, **5**, an isoelectronic and isostructural analogue of **4**, from reaction between Cp^*ReCl_4 and BH_3.THF.[22]

Experimental Section

General Methods. All manipulations were carried out under a dinitrogen or argon atmosphere using standard Schlenk line or drybox techniques. Toluene, pentane, and hexanes were distilled from sodium.[23] Starting materials Cp^*ReCl_4[24] and $(Cp^*WH_3)B_4H_8$[15] were prepared by published procedures. BH_3·THF (1 M) (Aldrich) was used as received without further purification.

NMR spectra were measured on a Varian-300 or Varian-500 FT-NMR at room temperature in C_6D_6 solutions unless otherwise noted. Residual protons of the solvent were used for reference in ^{1}H NMR experiments (δ, ppm: benzene 7.15; toluene, 2.09). A sealed tube containing $[NMe_4][B_3H_8]$ (δ, ppm −29.7) was used as the external reference to ^{11}B NMR experiments. Coupling constants are given in hertz. Infrared spectra were measured on a Nicolet 205 FT-IR spectrometer. Mass spectra were measured on a JEOL JMS-AX 505HA mass spectrometer using FAB (NBA matrix) mode. Perfluorokerosene was used as the standard for FAB high-resolution mass spectra. Elemental analysis was performed by M-H-W Laboratories, Phoenix, AZ.

$(Cp^*W)_3(\mu\text{-}H)B_8H_8$, 3. In a typical experiment a solution of $Cp^*H_3WB_4H_8$ (120 mg, 0.32 mmol, in 5 mL toluene) was heated to 110 °C for 30 min in a sealed Young's tube, after which ^{11}B NMR revealed that most of the starting material had been consumed and that the major product was $(Cp^*W)_2B_5H_9$, **2**. Purification by preparative thin-layer chromatography (toluene/hexane, 1:2) afforded four bands: yellow, R_f = 0.7, $(Cp^*W)_2B_5H_9$, **2** (40 mg, 45%); orange, R_f = 0.5, $(Cp^*W)_2B_7H_9$, **4**; apricot, R_f = 0.45, $Cp^*_3W_3(\mu\text{-}H)B_8H_8$, **3** (30 mg, 27%); and an unidentified brown band. Crystals suitable for X-ray diffraction were obtained by slow evaporation of a hexane solution of **3**.

(14) Bullick, H. J.; Grebenik, P. D.; Green, M. L. H.; Hughes, A. K.; Leach, J. B.; McGowan, P. C. *J. Chem. Soc., Dalton Trans.* **1995**, 67.
(15) Weller, A. S.; Shang, M.; Fehlner, T. P. *Organometallics* **1999**, *18*, 53.
(16) Wigley, D. E.; Gray, S. D. In *Comprehensive Organomet. Chem. II*; Abel, E. W., Stone, F. G. A., Wilkinson, G., Eds.; Pergamon: New York, 1995; Vol. 5.
(17) Morris, M. J. In *Comprehensive Organomet. Chem. II*; Abel, E. W., Stone, F. G. A., Wilkinson, G., Eds.; Pergamon: New York, 1995; Vol. 6.
(18) Gibson, V. C.; Bercaw, J. E.; Bruton, W. J., Jr.; Sanner, R. D. *Organometallics* **1986**, *5*, 976.
(19) Green, M. L. H. *Pure Appl. Chem.* **1978**, *50*, 27.
(20) Cloke, F. G. N.; Day, J. P.; Green, J. C.; Morley, C. P.; Swain, A. C. *J. Chem. Soc., Dalton Trans.* **1991**, 789.
(21) Weller, A. S.; Shang, M.; Fehlner, T. P. *J. Am. Chem. Soc.* **1998**, *120*, 8283.
(22) Weller, A. S.; Shang, M.; Fehlner, T. P. *Chem. Commun.* **1998**, 1787.
(23) Shriver, D. F.; Drezdzon, M. A. *The Manipulation of Air-Sensitive Compounds*, 2nd ed.; Wiley-Interscience: New York, 1986.
(24) Hermann, W. A.; Herdtweck, E.; Flöel, M.; Kulpe, J.; Kusthardt, U.; Okuda, J. *Polyhedron* **1987**, *6*, 1165.

Table 1. Crystal Data and Structure Refinement for 3, 4, and 5

	3	4	5
empirical formula	$C_{30}H_{54}B_8W_3$	$C_{20}H_{39}B_7W_2$	$C_{20}H_{37}B_7Re_2$
fw	1052.76	722.88	725.57
cryst syst	orthorhombic	monoclinic	tetragonal
space group	$Cmc2_1$	$P2_1/n$	$P4_2bc$
a (Å)	17.8507(13)	8.8158(17)	23.750(3)
b (Å)	14.1146(12)	18.068(5)	23.750(3)
c (Å)	13.7229(12)	16.623(4)	9.0035(7)
β		101.34(3)	
volume (Å)	3457.6(5)	2596.0(11)	5078.7(10)
Z	4	4	8
D_c (Mg/m^3)	2.022	1.850	1.898
F(000)	1984	1368	2736
wavelength (Å)	0.71073	0.71073	0.71073
abs coeff (mm$^{-1)}$	9.976	8.860	9.530
cryst size (mm)	0.23 × 0.19 × 0.08	0.40 × 0.32 × 0.03	0.11 × 0.10 × 0.10
temp (k)	293	293	293
diffractometer	Enraf-Nonius CAD4	Enraf-Nonius CAD4	Enraf-Nonius FAST
θ range, deg	2.28−25.01	2.25−25.00	2.43−28.36
no. of data collected	3155	4832	30128
no. of unique data	3155	4525	5079
no. of unique obsd data [$I > 2\sigma(I)$]	3076	3835	3870
abs corr	ψ scans	DIFABS	
max. and min. transmission	1.0000 and 0.4404	0.7770 and 0.1257	
refinement method	SHELXL-93	SHELXL-97	SHELXL-97
weighting scheme	σ weight	σ weight	σ weight
no. of data/restraints/params	3154/10/220	4525/8/277	5079/1/263
goodness-of-fit on F^2	1.061	1.065	1.105
Final R indices [$I > 2\sigma(I)$][a] (wR^2)[b]	0.0349 (0.0929)	0.0492 (0.1337)	0.0388 (0.0855)
R indices (all data)	0.0363 (0.1000)	0.0569 (0.1393)	0.0609 (0.0963)
max./min. residual e density	1.171/−1.619	1.732/−1.097	1.601/−1.872

[a] $R = \sum||F_o| - |F_c||/\sum|F_o|$. [b] $wR^2 = [\sum w(F_o^2 - F_c^2)^2/(w|F_o|^2)^2]^{1/2}$.

Spectroscopic Data for 3: ^{11}B NMR (toluene-d_8, δ ppm, J(BH)): 94.3 (1 B, d, 128), 82.5 (4 B, br, overlapping resonances), 24.1 (2 B, d, 128), −22.7 (1 B, br). ^{1}H NMR (toluene-d_8, 80 °C, δ ppm, J(BH)): 10.21 (1 BH_t, q, 129), 9.43 (2 BH_t, q, 125), 7.19 (2 BH_t, q, 130), 3.80 (2 BH_t, q, 129), 2.0 (2Cp*, s), 1.87 (1 Cp*, s), −2.64 (1 BH_t, partially collapsed quartet (pcq), ≈ 170), −15.34 [1 H, W−H−W, ^1J(WH) 67]. IR (KBr, $\nu(BH_t)$, cm^{-1}): 2527 m, 2480 m, 2432 m. MS (FAB+ in NBA), M^+ = 1055, 3 W, 8 B atoms, calcd for weighted average of isotopomers lying within the instrument resolution 1055.3596, obsd 1055.3560. Anal. Calcd for $C_{30}H_{54}B_8W_3$: C, 34.2; H, 5.17. Found: C, 34.1; H, 5.62.

$(Cp^*W)_2B_7H_9$, 4. As indicated immediately above, pyrolysis of **1** affords $(Cp^*W)_2B_7H_9$ in low yield (≈5% by NMR), but preparative thin-layer chromatography has insufficient resolution to separate it completely from the larger quantity of $(Cp^*W)_3(\mu\text{-H})B_8H_8$, **3**. However, photolysis at 280 nm of a C_6D_6 solution of $Cp^*WH_3B_4H_8$ (100 mg, 0.269 mmol) in a quartz tube until all of **1** had disappeared (≈6 days) affords a mixture of only **2** and **4**. Separation by preparative thin-layer chromatography (toluene/hexane, 1:4) affords **2** and pure **4** in 52 and 7% (7 mg) yields, respectively. However, crystals suitable for an X-ray diffraction study were in fact grown by slow evaporation of a hexane solution of a mixture **3** and **4**.

Spectroscopic Data for 4. ^{11}B NMR (δ ppm, J(BH)): δ 99.0 (1 B, d, 147), 83.5 (2 B, d, 153), 46.6 (2 B, d, 158), 17.6 (2 B, d, 136). ^{1}H NMR (δ ppm, J(BH)): δ 10.40 (2 BH_t, pcq, 146), 10.15 (1 BH_t, pcq, 143), 5.98 (2 BH_t, pcq, 156), 2.23 (2 BH_t, pcq, 136), 2.04 (2 Cp*, s), −8.88 (2 μ_3-H, br s). IR (KBr, $\nu(BH_t)$, cm^{-1}): 2505 m, 2492 m. MS (FAB+ in NBA), M^+ = 723 2 W, 7 B, 20 C atoms, calcd for weighted average of isotopomers lying within the instrument resolution 723.2785, obsd 723.2773. Anal. Calcd for $C_{20}H_{39}B_7W_2$: C, 33.2; H, 5.44. Found: C, 33.9; H, 5.31.

$(Cp^*Re)_2B_7H_7$, 5. Cp^*ReCl_4 (60 mg, 0.130 mmol) was suspended in 10 mL of toluene, and BH_3·THF (6 equiv) was added. The resulting green homogeneous solution was stirred at room temperature for 16 h and then heated to 45 °C in toluene for 8 h. Removal of volatiles in vacuo and purification by preparative thin-layer chromatography (toluene/hexane, 1:2) affords moderately air-stable, pale yellow, $(Cp^*Re)_2B_7H_7$, **5** (36 mg, 76%). Crystals suitable for X-ray diffraction were grown by slow evaporation of a hexane solution of **5**.

Spectroscopic Data for 5. ^{11}B NMR (δ ppm, J(BH)): 101.7 (1 B, d, 169), 85.6 (2 B, d,164), 82.1 (2 B, d, 164), 3.6 (2 B, d, 166). ^{1}H NMR (δ ppm, J(BH)): 11.21 (pcq), 2 BH_t (162)], 10.12 [pcq, 1 BH_t (167)], 8.63 [pcq, 2 BH_t (173)], 1.92 (s, 30 H, Cp*), −0.04 (pcq, 2 BH_t (166)]. IR (KBr, $\nu(BH_t)$, cm^{-1}): 2515 m, 2490 m. MS (FAB+ in NBA), M^+ = 728, 2 Re, 7 B, 20 C atoms, calcd for weighted average of isotopomers lying within the instrument resolution 728.2662, obsd 728.2676. Anal. Calcd for $C_{20}H_{37}B_7Re_2$: C, 33.1; H, 5.14. Found: C, 33.4; H, 5.40.

X-ray Structure Determinations. $(Cp^*W)_3(\mu\text{-H})B_8H_8$, 3. Diffraction data were collected at a temperature of 20 °C on an Enraf-Nonius CAD4 diffractometer. XCAD4 software was used to process intensity data on a PC-Linux platform.[25] An empirical absorption correction based on a series of ψ scans, structure solution, and refinement was performed on a PC by using the SHELXTL package.[26] After all non-hydrogen atoms were refined anisotropically, difference Fourier synthesis located all hydrogen atoms. In the final refinement cyclopentadienyl hydrogen atoms were refined with an idealized riding model. The hydride was refined isotropically with the isotropic thermal parameter fixed to 1.2 times the equivalent isotropic thermal parameter of its bonded W atom. The rest of the borane hydrogen atoms were refined isotropically with bond length restraints. The polarity of the c-axis was determined by a practical zero value of the Flack absolute structure parameter, 0.01(3).[27] Detailed crystallographic information is given in Table 1, and the structural data have been archived.[21]

$(Cp^*W)_2B_7H_9$, 4. Data collection, data reduction, structure solution, and refinement were performed in the same manner as **3**. An empirical absorption correction based on a series of

(25) Harms, K. In IUCr SInCris Software; 1996.
(26) Sheldrick, G. M. *SHELXTL*; In Siemens Industrial Automation Inc.: Madison, WI, 1994.
(27) Flack, H. D. *Acta Crystallogr.* **1983**, *A39*, 876.

ψ scans failed for the irregular platelike crystal with laminar surface indexes (1,0,1), while DIFABS not only found the right laminar surface but also gave reasonable correction. In the final refinement cyclopentadienyl and most of the terminal borane hydrogen atoms were refined with idealized riding models. The two capping hydrogen atoms and the two terminal hydrogen atoms were refined with bond length restraints. Detailed crystallographic information is given in Table 1, and the structural data have been archived.[22]

$(Cp^*Re)_2B_7H_7$, 5. Single-crystal crystallographic experiments were carried out on an Enraf-Nonius FAST area detector diffractometer at 293 K by methods and procedures for small molecules described in the literature.[28] Except for averaging a large number of redundant data sets for a 4/*mmm* point group, no other absorption correction was applied. Structure solution and refinement were performed on a PC by using the SHELXTL package in the same way as for **3**.[26] In the final refinement hydrogen atoms were refined with idealized riding models. The polarity of the *c*-axis was determined by a near zero value of the Flack absolute structure parameter, −0.04(2).[27] Detailed crystallographic information is given in Table 1, and the structural data have been archived.[22]

MO Calculations. The molecular orbital calculations were carried out on $Cp^*_3W_3(\mu\text{-H})B_8H_8$, **3**, $(Cp^*W)_2B_7H_9$, **4**, $(Cp^*Re)_2B_7H_7$, **5**, using the Fenske−Hall approximate MO method.[29,30] This method is a proven, nonparametrized MO method often used to characterize the electronic structure of complex systems. The 1988 version for Macintosh computers utilizing a minimal basis set was employed. The η^5-C_5H_5 ligand was used in place of the η^5-C_5Me_5 ligand found in the actual compounds for simplicity. The structures of the three compounds are schematically shown in Chart 1. Coordinates were taken from the X-ray crystallographic data for the Cp* derivatives and idealized where appropriate. For the hypothetical structure of **5** in the form of a distorted tricapped trigonal prism, the closest fit incorporating reasonable Re−B and B−B distances was used. No claim for uniqueness is made.

Results and Discussion

Synthesis. Pyrolysis of **1** results in three major products: $(Cp^*W)_2B_5H_9$, **2**, $(Cp^*W)_3(\mu\text{-H})B_8H_8$, **3**, and $(Cp^*W)_2B_7H_9$, **4** (Chart 1). Compound **2**, characterized as a bicapped trigonal bipyramidal cluster, is formed in greatest yield but is better synthesized from the reaction between Cp^*WCl_4 and BH_3·THF.[15] The yield of **3** is sensitive to pyrolysis conditions. Both **3** and **4** have similar R_f values, and **4**, always present in lower amount than **3**, cannot be cannot be isolated free from **3**. Fortunately, the photolysis of **1** forms only **2** and **4**, permitting the isolation of the latter as a pure substance. For comparison note that two compounds formally analogous to **1** behave very differently when heated. $Cp^*TaCl_2B_4H_8$, with a 16-electron Ta center, sublimes without decomposition,[11] and 2-$CpCoB_4H_8$ rearranges to 1-$CpCoB_4H_8$ on heating to higher temperatures than employed here.[31]

$(Cp^*W)_3(\mu\text{-H})B_8H_8$, 3. The molecular structure of **3** is shown in Figure 1, with selected bond lengths and angles given in Table 2. As can be seen, **3** displays an unusual structural motif. It is constructed from a triangle of W atoms implanted into a complex ring of eight boron atoms. In the solid state it has crystallographically imposed C_s symmetry, meaning that two of the {WCp*} groups are equivalent, while the boron atoms are arranged so that there are three pairs of equivalent boron atoms and two unique vertexes. All cage hydrogen atoms were located and refined from the difference map, including a W−H−W group [H(1)], the positioning of which was confirmed by ^{1}H NMR spectroscopy (see below). All of the B−B, B−W, and W−W distances lying on the cluster surface correspond to bonding interactions. The W−W cross cluster distance, W(1)−W(2) (3.0597(6) Å), is 0.26 Å longer than the hydrogen-bridged W−W distance. However, this distance falls within the range reported previously for complexes with $\{(\eta^5\text{-}C_5R_5)W\}_3$ triangles, such as $(Cp^*W)_3(CO)_6(\mu_3\text{-PS})$[32] [W−W 3.109(2)−3.153(2) Å] or $\{(\eta^5\text{-}C_5H_4Me)W(CO)_2\}_3Co(CO)_3$[33] [W−W 2.9580−2.9526 Å], both of which are described as electron precise in valence bond terms and formally have W−W single bonds. This justifies considering all W−W distances as bonding. The approximate MO calculations, described below, support this description.

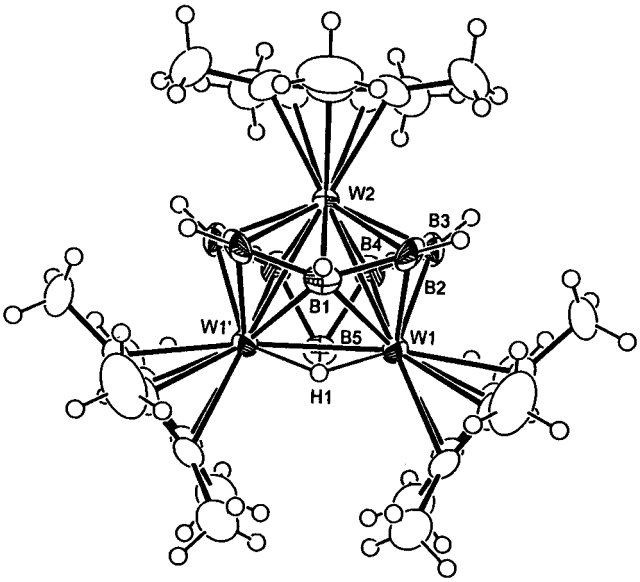

Figure 1. Molecular structure of $Cp^*_3(\mu\text{-H})W_3B_8H_8$, **3**.

Consistent with retention of a mirror plane of symmetry in solution, the $^{11}B\{^1H\}$ NMR spectrum of **3** shows four resonances in the ratio 1:4 (2 + 2 coincidence): 2:1, at δ 94.3, 82.5, 24.1, and −22.7, respectively. With the exception of the highest field signal, all are sensible doublets in the coupled spectrum. The former is so broad (fwhm ≈ 400 Hz coupled; ≈ 300 Hz $\{^1H\}$) that its multiplicity is hidden. The wide chemical shift range of the resonances, which is rarely observed in metallaboranes species,[34] is consonant with the unusual solid-state structure described above.

The ^{1}H NMR spectrum of **3** also supports the solid-state structure. Two signals, in a 1:2 ratio, are observed for the Cp* methyl groups, while resonances due to five BH_t groups in the ratio of 1:2:2:2:1 are observed. In the high-field region of the ^{1}H NMR spectrum a single, sharp integral 1 H, resonance is observed at δ −15.34

(28) Scheidt, W. R.; Turowska-Tyrk, I. *Inorg. Chem.* **1994**, *33*, 1314.
(29) Hall, M. B.; Fenske, R. F. *Inorg. Chem.* **1972**, *11*, 768.
(30) Fenske, R. F. *Pure Appl. Chem.* **1988**, *27*, 61.
(31) Venable, T. L.; Sinn, E.; Grimes, R. N. *J. Chem. Soc., Dalton Trans.* **1984**, 2275.
(32) Davies, J. E.; Mays, M. J.; Pook, E. J.; Raithby, P. R.; Tompkin, P. K. *Chem. Commun.* **1997**, 1997.
(33) Chetcuti, M. J.; Gordon, J. C.; Fanwick, P. E. *Inorg. Chem.* **1990**, *29*, 3781.
(34) Housecroft, C. E. *Adv. Organomet. Chem.* **1991**, *33*, 1.

Table 2. Selected Bond Distances (Å) and Bond Angles (deg) for 3

W(1)−B(3)	2.077(13)	W(2)−B(2)#1	2.231(10)
W(1)−B(2)	2.16(2)	W(2)−B(2)	2.231(10)
W(1)−B(5)	2.226(13)	W(2)−B(3)	2.254(12)
W(1)−B(4)	2.331(12)	W(2)−B(3)#1	2.254(12)
W(1)−B(1)	2.52(2)	W(2)−B(1)	2.26(2)
W(1)−W(1)#1	2.8008(7)	W(2)−B(4)	2.339(13)
W(1)−W(2)	3.0597(6)	W(2)−B(4)#1	2.339(13)
W(1)−H(1)	1.58(7)	B(3)−H(31)	1.10(7)
B(1)−B(2)	1.71(2)	B(4)−B(5)	1.78(2)
B(1)−B(2)#1	1.71(2)	B(4)−B(4)#1	1.79(2)
B(1)−W(1)#1	2.52(2)	B(4)−H(41)	1.10(7)
B(1)−H(11)	1.12(7)	B(5)−B(4)#1	1.78(2)
B(2)−B(3)	1.83(2)	B(5)−W(1)#1	2.226(13)
B(2)−H(21)	1.10(8)	B(5)−H(51)	1.11(8)
B(3)−B(4)	1.75(2)		

B(3)−W(1)−B(2)	51.2(6)	B(1)−W(2)−B(4)#1	101.8(6)
B(3)−W(1)−B(5)	92.1(6)	B(4)−W(2)−B(4)#1	44.9(6)
B(2)−W(1)−B(5)	122.0(5)	B(2)−B(1)−B(2)#1	132.6(13)
B(3)−W(1)−B(4)	46.3(5)	B(2)−B(1)−W(2)	66.6(6)
B(2)−W(1)−B(4)	87.0(5)	B(2)#1−B(1)−W(2)	66.6(6)
B(5)−W(1)−B(4)	45.8(5)	B(2)−B(1)−W(1)	57.7(7)
B(3)−W(1)−B(1)	83.6(5)	B(2)#1−B(1)−W(1)	118.9(11)
B(2)−W(1)−B(1)	42.1(5)	W(2)−B(1)−W(1)	79.3(5)
B(5)−W(1)−B(1)	101.1(4)	B(2)−B(1)−W(1)#1	118.9(11)
B(4)−W(1)−B(1)	94.7(5)	B(2)#1−B(1)−W(1)#1	57.7(7)
B(3)−W(1)−W(1)#1	107.9(3)	W(2)−B(1)−W(1)#1	79.3(5)
B(2)−W(1)−W(1)#1	94.5(3)	W(1)−B(1)−W(1)#1	67.5(5)
B(5)−W(1)−W(1)#1	51.0(3)	B(1)−B(2)−B(3)	120.6(10)
B(4)−W(1)−W(1)#1	77.5(3)	B(1)−B(2)−W(1)	80.2(9)
B(1)−W(1)−W(1)#1	56.3(3)	B(3)−B(2)−W(1)	62.0(6)
B(3)−W(1)−W(2)	47.4(3)	B(1)−B(2)−W(2)	68.5(6)
B(2)−W(1)−W(2)	46.8(3)	B(3)−B(2)−W(2)	66.5(5)
B(5)−W(1)−W(2)	75.2(5)	W(1)−B(2)−W(2)	88.2(5)
B(4)−W(1)−W(2)	49.2(3)	B(4)−B(3)−B(2)	119.5(8)
B(1)−W(1)−W(2)	46.6(4)	B(4)−B(3)−W(1)	74.5(6)
W(1)#1−W(1)−W(2)	62.762(8)	B(2)−B(3)−W(1)	66.8(6)
B(2)#1−W(2)−B(2)	89.5(8)	B(2)−B(3)−W(2)	65.2(5)
B(2)#1−W(2)−B(3)	127.5(5)	W(1)−B(3)−W(2)	89.8(4)
B(2)−W(2)−B(3)	48.3(5)	B(3)−B(4)−B(5)	123.1(9)
B(2)#1−W(2)−B(3)#1	48.3(5)	B(3)−B(4)−B(4)#1	130.9(5)
B(2)−W(2)−B(3)#1	127.5(5)	B(5)−B(4)−B(4)#1	59.8(5)
B(3)−W(2)−B(3)#1	129.6(7)	B(3)−B(4)−W(1)	59.2(5)
B(2)#1−W(2)−B(1)	44.9(4)	B(5)−B(4)−W(1)	64.0(6)
B(2)−W(2)−B(1)	44.9(4)	B(4)#1−B(4)−W(1)	102.5(3)
B(3)−W(2)−B(1)	86.2(4)	B(3)−B(4)−W(2)	65.1(6)
B(3)#1−W(2)−B(1)	86.2(4)	B(5)−B(4)−W(2)	105.5(7)
B(2)#1−W(2)−B(4)	117.1(5)	B(4)#1−B(4)−W(2)	67.5(3)
B(2)−W(2)−B(4)	85.3(5)	W(1)−B(4)−W(2)	81.9(4)
B(3)−W(2)−B(4)	44.7(5)	B(3)−B(4)−H(41)	106(5)
B(3)#1−W(2)−B(4)	88.9(5)	B(4)−B(5)−B(4)#1	60.4(10)
B(1)−W(2)−B(4)	101.8(6)	B(4)−B(5)−W(1)#1	107.1(9)
B(2)#1−W(2)−B(4)#1	85.3(5)	B(4)#1−B(5)−W(1)#1	70.2(6)
B(2)−W(2)−B(4)#1	117.1(5)	B(4)−B(5)−W(1)	70.2(6)
B(3)−W(2)−B(4)#1	88.9(5)	B(4)#1−B(5)−W(1)	107.1(9)
B(3)#1−W(2)−B(4)#1	44.7(5)	W(1)#1−B(5)−W(1)	78.0(6)

and is assigned to the W−H−W hydride. Observation of two sets of ^{183}W satellites associated with this signal confirms the positioning of the bridging hydride in the solid-state structural determination. A doublet, ^1J(WH) 67, of relative intensity 31% due to ^{183}W−H−W isotopomer (calcd intensity 33%) and the outer lines of a triplet of relative intensity 3% due to the ^{183}W−H−^{183}W isotopomer (calcd 2.7%) unambiguously place this hydride as bridging two W centers.

The correlation and assignment of the ^{1}H and ^{11}B resonances provide additional corroboration of the unusual character of **3**. The proton resonances have been assigned to specific resonances in the ^{11}B NMR spectrum by ^{1}H{^{11}B selective} experiments. A plot of ^{1}H shifts vs ^{11}B shifts is approximately linear. Initially the broad integral 1 ^{1}H resonance at δ −2.64 caused problems in interpretation, as it is in a chemical shift range normally associated with B−H−B hydrogens. However, (a) there are no other signals that could be assigned to a B−H terminal resonance; (b) this high-field signal is shown to be coupled exclusively to the boron associated with the resonance at δ(^{11}B) −22.7; and (c) the ^{1}H NMR spectrum of **3** at +80 °C[35] resolved the signal into a partially collapsed quartet with J(BH) ≈170. All observations confirm that this high-field resonance corresponds to a terminal hydrogen in an unusual local electronic environment with high asymmetry.

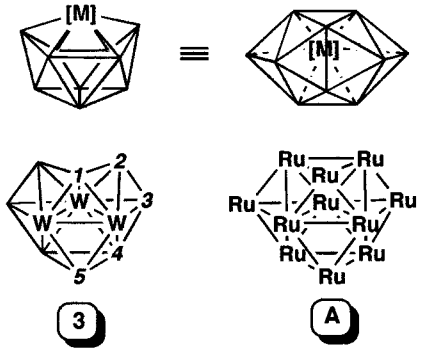

Figure 2. Comparison of the structures of **3** with a standard MB_{10} cage cluster geometry (top) and the close packed $[Ru_{11}H(CO)_{27}]^{3-}$, **A**. Exo-cluster ligands have been omitted for clarity.

Especially interesting are the two unique proton and boron resonances, which bookend the shift ranges, $\Delta(\delta^1\text{H}) = 12.8$ and $\Delta(\delta^{11}\text{B}) = 117$. These two unique B−H fragments, B(1) and B(5), have differing connectivities in the cluster. B(1) is joined to 3 W and 2 B atoms in a fairly asymmetric fashion, e.g., W(2)−B(1) = 2.26(2) Å vs W(1,1′)−B(1) = 2.52(2) Å, whereas B(5) is joined to 2 W and 2 B atoms. Connectivity/chemical shift correlations have been used in metallaborane chemistry previously, with low connectivity vertexes often appearing at low field, especially when also adjacent to a metal center.[36] On the basis of ^{11}B peak width and structure connectivities, B(1) resonates at δ −22 and B(5) at δ 94. Further, there are two five-connected environments, B(1) and B(4), and three four-connected environments, B(2), B(3), and B(5). This permits assignment of the chemical shifts in the ^{11}B NMR spectrum of **3**: three low-field resonances (one a 2 + 2 coincidence) with the three four-connected vertexes, and two high-field resonances with the two five-connected boron atoms. The final assignment is δ 94.3, B(5); 82.5, B(2,3); 24.1, B(4); and −22.7, B(1).

Structure and Bonding of 3. The structure observed for **3** is not that expected for an 11-vertex metallaborane, e.g., that based on an octadecahedron (Figure 2). Although known 11-vertex closed monometallaboranes exhibit the expected geometry (Figure 2) and the 12 sep required by the electron counting rules,[37] examples of 11-fragment closed clusters with 11

(35) Kidd, R. G. In *NMR of Newly Accessible Nuclei*; Laszlo, P., Ed.; Academic Press: New York, 1983; Vol. 2, p 49.
(36) Coldicott, R. S.; Kennedy, J. D.; Thornton-Pett, M. *J. Chem. Soc., Dalton Trans.* **1996**, 3819.
(37) Kennedy, J. D. In *The Borane, Carborane, Carbocation Continuum*; Casanova, J., Ed.; Wiley: New York, 1998; p 85.

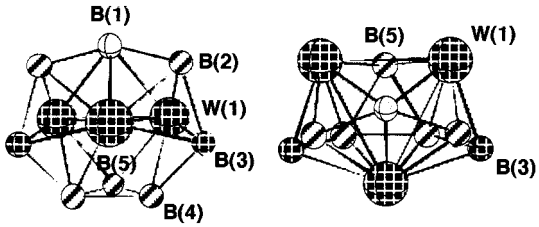

Figure 3. Ball and stick representation of **3** (spheres of arbitrary radius), showing views parallel (left) and perpendicular (right) with the plane of the W_3 triangle. Hatched, solid, and white spheres indicate notional A, B, and C layers, respectively.

sep are also described in the literature.[38,39] Depending on the point of view adopted, they constitute examples of "hypercloso"[40] or "isocloso clusters".[41] In the case of 10-vertex clusters, an observable structural change distinguishes hypercloso $(C_6H_6)RuB_9H_9$ with 10 sep and closo $[(C_6H_6)RuB_9H_9]^{2-}$ with 11 sep. The recent demonstration that these two clusters interconvert by the addition and removal of two electrons unambiguously establishes the existence of *n* sep hypercloso clusters.[42] It also hints that a solution to the problem presented by **3** may be found in an examination of known high nuclearity metal clusters with formal sep counts less than *n*.

Comparison of the stick diagrams in Figure 2 shows a structural resemblance between **3** and the 11-atom transition metal cluster $[Ru_{11}H(CO)_{27}]^{3-}$, **A**,[43] which exhibits a hexagonal close packed metal core, with distinct A, B, A layers. For both **3** and **A**, the bottom two layers can be derived from the A, B layers of a hexagonal close packed structure, B(3) and B(3′) lying somewhat below (0.511(4) Å) the plane of the W_3 triangle. The top layer in **A** is positioned to afford A, B, A stacking (hexagonal close packed), as are boron atoms B(2) and B(2′) in **3**. However, B(1) is in a position that lies above the center of the B(4), B(4′), B(5) triangle, and so corresponds to A, B, C stacking (cubic close packed), like that seen in $[Os_{10}H_4(CO)_{24}]^{2-}$.[44] This means that in the top layer there is a difference in the positioning of the connectivities around B(1) and B(2,2′) and their positional equivalents in **A**; that is B(1) has an additional connection to the second layer, and B(2,2′) are not connected (Figure 3). However, the total number of connectivities in the two compounds is the same.

That there are two different forms of stacking evident is due to the disparity in the atomic radii between W and B (Figure 3). For spheres of equal radii an arrangement of the type found in **3** is not possible but is adopted as it permits B(1)−B(2,2′) bonding in the third layer. Likewise, the deviation of B(3,3′) from coplanarity with the W_3 triangle allows B−B bonding between B(3,3′) and both B(2,2′) and B(4,4′).

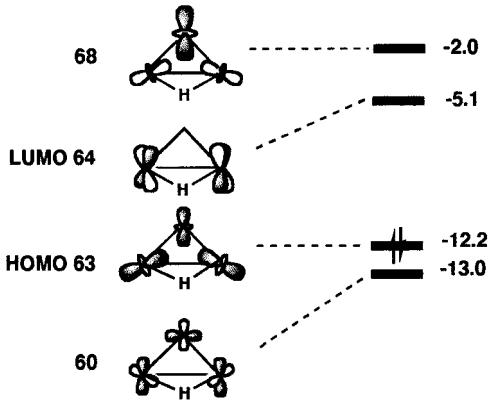

Figure 4. Simplified Fenske−Hall MO diagram for **3** in which only the W_3 triangle is shown. MOs 63 and 68 illustrate one filled bonding Walsh orbital and one unfilled antibonding Walsh orbital, respectively.

The analysis of geometry in terms of a close packed array of metal and boron atoms justifies the observed cluster electron count. **A** possesses 146 cve, consistent with MO calculations carried out on high-nuclearity metal clusters of various shapes.[45] Note that condensed structures with 10 or more metal atoms often deviate from a simple sep or cve count. Compound **A** has 146 cve, while conventional application of the counting rules suggests 144. The cluster $[Os_{20}(CO)_{40}]^{2-}$[46] has 242 cve, while theory predicts 248 cve. Therefore, we use the *observed* cve of **A** to establish the *expected* count for **3**. A M_3B_8 cluster with a geometry identical to **A** should have $146 - (8 \times 10)$ cve, i.e., 66.[5,47] Compound **3** has 66 cve.

Electron counting arguments do not establish whether the proposed electron count is actually suitable for the observed structure nor does it define the bonding factors leading to the evident stability of the compound. A simplified MO scheme for **3** based on Fenske−Hall calculations[29,30] is shown in Figure 4. Apparent is the substantial HOMO−LUMO gap, consistent with molecular stability at the observed electron count. Moreover, the HOMO, at −12.2 eV, is W−W bonding consisting of a symmetric bonding combination of all three W d_{z^2} orbitals which point to the center of the W_3 isosceles triangle. This is analogous to the a_1' in-plane C−C bonding Walsh orbital of cyclopropane. The MOs corresponding to the e′ Walsh orbitals are found at −15.2 and −15.5 eV, being stabilized and split by the bridging hydrogen atom. The corresponding, unoccupied MOs analogous to the antibonding Walsh orbitals of e′ and a_2' symmetries are found at −3.1, −2.0 (shown), and 2.5 eV, respectively. The Mulliken overlap for W(1)−W(2) is 0.08, which compares favorably with that found for **2**, 0.13, which has a W−W separation of 2.8170(8) Å.[15] Clearly, the cross-cage W(1,1′)−W(2) interactions, which distinguish **3** from a single cage species, as well as the close packed arrangement of atoms, are essential to its stability. Without the former bonding interactions there would be at least one low-lying unfilled empty orbital.

(38) Fowkes, H.; Greenwood, N. N.; Kennedy, J. D.; Thornton-Pett, M. *J. Chem. Soc., Dalton Trans.* **1986**, 517.
(39) Brown, M.; Fontaine, X. L. R.; Greenwood, N. N.; Kennedy, J. D.; Thornton-Pett, M. *J. Chem. Soc., Dalton Trans.* **1990**, 3039.
(40) Baker, R. T. *Inorg. Chem.* **1986**, *25*, 109.
(41) Kennedy, J. D. *Inorg. Chem.* **1986**, *25*, 111.
(42) Littger, R.; Spencer, J. T. In *Boron USA-VI*; Athens, GA, 1998.
(43) Bailey, P. J.; Beswick, M. A.; Johnson, B. F. G.; Lewis, J.; Raithby, P. R.; Ramirez de Arellano, M. C. *J. Chem. Soc., Dalton Trans.* **1992**, 3159.
(44) Braga, D.; Lewis, J.; Johnson, B. F. G.; McPartlin, M.; Nelson, W. J. H.; Vargas, M. D. *J. Chem. Soc., Chem. Commun.* **1983**, 241.
(45) Ciani, G.; Sironi, A. *J. Organomet. Chem.* **1980**, *197*, 233.
(46) Amoroso, A. J.; Johnson, B. F. G.; Lewis, J.; Raithby, P. R.; Wong, W. T. *Angew. Chem., Int. Ed. Engl.* **1991**, *30*, 1505.
(47) Mingos, D. M. P. In *Inorganometallic Chemistry*; Fehlner, T. P., Ed.; Plenum: New York, 1992; p 179.

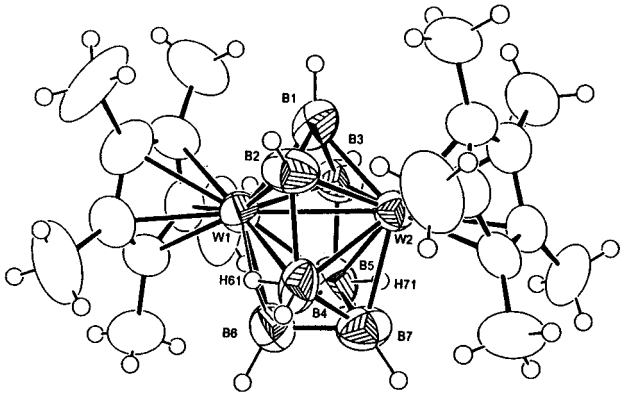

Figure 5. Molecular structure of $(Cp^*W)_2B_7H_9$, **4**.

Having established *a postori* that the structure of **3** is reasonable on the basis of metal cluster precedents, one wonders if existing electron counting theory accommodates this compound. Mingos and Wales treat the complex behavior of high-nuclearity clusters[5] in terms of three types: (1) cluster bonding governed by inner cluster count with radial interactions predominant; (2) cluster bonding governed by outer cluster count where radial and tangential interactions are important; and (3) cluster bonding intermediate between these two situations. Situation 1 corresponds to multiple capping in which the outer cluster emulates the ligands of a single cluster and the count for an all metal cluster is $12n_s + \Delta_i$, where n_s is the number of surface fragments and Δ_i is the count characteristic of the inner triangle. Situation 2 pertains, for example, to clusters containing interstitial fragments. Compound **3** fits into the first category when viewed as a metal triangle capped by eight BH fragments, albeit the borane fragment hardly covers the large metal triangle. Because the inner deltahedron is a triangle, one additional orbital (a_2') can be stabilized such that it is accessible. Thus the count is $96 + 48 + 2 = 146$, implying a count of 66 for a M_3B_8 species. This analysis completes the connection between **3** and high-nuclearity metal clusters. It also relegates B−B bonding to a secondary role in terms of control of structure consistent with the fact that the borane fragement has little relationship to a typical polyhedral borane.

For all practical purposes, then, the Cp*W fragments do act as −1 cluster fragments in the sense of withdrawing cluster electrons from the borane fragment, thereby causing the framework to become highly condensed. Thus, **3** constitutes an example of a $(n - 4)$ sep highly condensed cluster. Note that **2** may be considered an example of a $(n - 1)$ cluster in that it possesses 7 cluster fragments and 6 sep. However, because of its small size, it is easily accommodated by the counting rules as a bicapped trigonal bipyramidal cluster. What about $(n - 2)$ or $(n - 3)$ clusters?

$(Cp^*W)_2B_7H_9$, 4. The molecular structure of **4** is shown in Figure 5, with selected bond lengths and angles given in Table 3. Immediately apparent is that **4** does not display the structural motif expected for a closed nine-vertex metallaborane, i.e., a tricapped trigonal bipyramid. In addition, the two W centers are separated by 2.9522(8) Å, falling in the range associated with W−W single bonds.[48] This provides convincing evidence of a cross-cage W−W bonding interaction. The boron atoms are arranged so that there are three pairs of equivalent atoms and one unique one. All B−B and W−B bond lengths are in the range normally associated with bonding interactions. The two μ_3-H atoms were located in the difference map, and their presence was confirmed by ^{1}H NMR spectroscopy (see below). More-

Table 3. Selected Bond Distances (Å) and Bond Angles (deg) for 4

W(1)−B(1)	2.154(14)	B(1)−B(3)	1.80(2)
W(1)−B(3)	2.160(12)	B(1)−B(2)	1.809(19)
W(1)−B(6)	2.209(15)	B(1)−H(1)	1.1000
W(1)−B(2)	2.268(14)	B(2)−B(4)	1.937(19)
W(1)−B(5)	2.285(14)	B(2)−H(2)	1.1000
W(1)−C(4)	2.328(12)	B(3)−B(5)	1.89(2)
W(1)−C(5)	2.353(10)	B(3)−H(3)	1.1000
W(1)−C(2)	2.369(11)	B(4)−B(7)	1.78(2)
W(1)−C(3)	2.371(11)	B(4)−B(6)	1.81(2)
W(1)−C(1)	2.382(11)	B(4)−H(4)	1.1000
W(1)−B(4)	2.441(15)	B(4)−H(61)	1.08(5)
W(1)−W(2)	2.9522(8)	B(5)−B(6)	1.75(2)
W(1)−H(61)	1.70(8)	B(5)−B(7)	1.81(2)
W(2)−B(2)	2.158(11)	B(5)−H(5)	1.1000
W(2)−B(1)	2.176(15)	B(5)−H(71)	1.09(5)
W(2)−B(7)	2.192(13)	B(6)−B(7)	1.74(2)
W(2)−B(3)	2.250(14)	B(6)−H(61)	1.08(5)
W(2)−B(4)	2.294(13)	B(6)−H(62)	1.09(5)
W(2)−B(5)	2.419(12)	B(7)−H(71)	1.09(5)
W(2)−H(71)	1.70(8)	B(7)−H(72)	1.09(5)

B(1)−W(1)−B(3)	49.4(6)	B(1)−W(1)−B(4)	87.2(5)
B(1)−W(1)−B(6)	120.7(5)	B(3)−W(1)−B(4)	95.9(5)
B(3)−W(1)−B(6)	95.1(6)	B(6)−W(1)−B(4)	45.4(5)
B(1)−W(1)−B(2)	48.2(5)	B(2)−W(1)−B(4)	48.4(5)
B(3)−W(1)−B(2)	87.0(5)	B(5)−W(1)−B(4)	67.8(5)
B(6)−W(1)−B(2)	93.5(5)	B(1)−W(1)−W(2)	47.3(4)
B(1)−W(1)−B(5)	90.0(5)	B(3)−W(1)−W(2)	49.3(4)
B(3)−W(1)−B(5)	50.2(5)	B(6)−W(1)−W(2)	73.4(4)
B(6)−W(1)−B(5)	45.7(5)	B(2)−W(1)−W(2)	46.6(3)
B(2)−W(1)−B(5)	97.4(4)	B(1)−B(3)−W(1)	65.1(6)
B(4)−W(1)−W(2)	49.2(3)	B(5)−B(3)−W(1)	68.3(6)
B(2)−W(2)−B(1)	49.3(5)	B(1)−B(3)−W(2)	63.8(6)
B(2)−W(2)−B(7)	97.4(5)	B(5)−B(3)−W(2)	70.9(6)
B(1)−W(2)−B(7)	121.3(5)	W(1)−B(3)−W(2)	84.0(4)
B(2)−W(2)−B(3)	87.5(5)	B(7)−B(4)−B(6)	58.2(8)
B(1)−W(2)−B(3)	48.0(5)	B(7)−B(4)−B(2)	123.1(9)
B(7)−W(2)−B(3)	93.4(5)	B(6)−B(4)−B(2)	121.1(10)
B(2)−W(2)−B(4)	51.5(5)	B(7)−B(4)−W(2)	63.7(6)
B(1)−W(2)−B(4)	90.5(5)	B(6)−B(4)−W(2)	99.3(8)
B(7)−W(2)−B(4)	46.7(5)	B(2)−B(4)−W(2)	60.6(5)
B(3)−W(2)−B(4)	97.7(5)	B(7)−B(4)−W(1)	96.4(8)
B(2)−W(2)−B(5)	96.5(5)	B(6)−B(4)−W(1)	60.5(6)
B(1)−W(2)−B(5)	86.1(5)	B(2)−B(4)−W(1)	61.1(6)
B(7)−W(2)−B(5)	46.0(5)	W(2)−B(4)−W(1)	77.1(4)
B(3)−W(2)−B(5)	47.5(5)	B(6)−B(5)−B(7)	58.7(8)
B(4)−W(2)−B(5)	68.1(5)	B(6)−B(5)−B(3)	125.0(10)
B(2)−W(2)−W(1)	49.8(4)	B(7)−B(5)−B(3)	121.7(9)
B(1)−W(2)−W(1)	46.7(4)	B(6)−B(5)−W(1)	64.9(7)
B(7)−W(2)−W(1)	74.7(4)	B(7)−B(5)−W(1)	101.1(7)
B(3)−W(2)−W(1)	46.7(3)	B(3)−B(5)−W(1)	61.5(6)
B(4)−W(2)−W(1)	53.7(4)	B(6)−B(5)−W(2)	96.6(8)
B(5)−W(2)−W(1)	49.1(3)	B(7)−B(5)−W(2)	60.4(5)
B(3)−B(1)−B(2)	115.2(10)	B(3)−B(5)−W(2)	61.5(6)
B(3)−B(1)−W(1)	65.5(6)	W(1)−B(5)−W(2)	77.7(4)
B(2)−B(1)−W(1)	69.2(6)	B(7)−B(6)−B(5)	62.6(8)
B(3)−B(1)−W(2)	68.1(7)	B(7)−B(6)−B(4)	60.1(8)
B(2)−B(1)−W(2)	64.8(6)	B(5)−B(6)−B(4)	96.0(9)
W(1)−B(1)−W(2)	86.0(5)	B(7)−B(6)−W(1)	106.5(7)
B(1)−B(2)−B(4)	115.8(9)	B(5)−B(6)−W(1)	69.5(7)
B(1)−B(2)−W(2)	65.8(6)	B(4)−B(6)−W(1)	74.1(7)
B(4)−B(2)−W(2)	67.9(6)	B(6)−B(7)−B(4)	61.7(8)
B(1)−B(2)−W(1)	62.6(6)	B(6)−B(7)−B(5)	58.7(8)
B(5)−W(1)−W(2)	53.2(3)	B(4)−B(7)−B(5)	94.6(9)
B(4)−B(2)−W(1)	70.5(6)	B(6)−B(7)−W(2)	105.3(8)
W(2)−B(2)−W(1)	83.6(4)	B(4)−B(7)−W(2)	69.7(6)
B(1)−B(3)−B(5)	116.6(9)	B(5)−B(7)−W(2)	73.6(6)

(48) Rheingold, A. L.; Harper, J. R. *Acta Crystallogr.* **1991**, *C47*, 184.

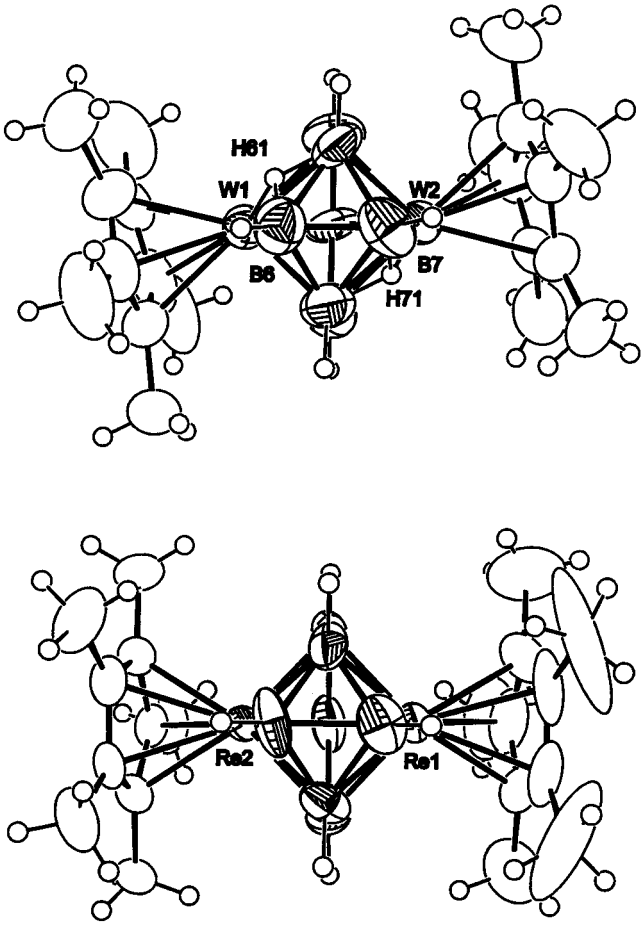

Figure 6. Comparison of the molecular structures of $(Cp^*W)_2B_7H_9$, **4**, and $(Cp^*Re)_2B_7H_7$, **5**.

over, their positioning on the cluster surface is given extra weight by the response of the Cp* groups. The two bridging hydrogen atoms, H(61) and H(71), are located on the W(1)−B(4)−B(6) and W(2)−B(5)−B(7) faces, respectively, so as to give the molecule approximate C_2 symmetry, the two Cp* groups tilted from the B(6)−B(7)−W(1)−W(2)−B(1) plane by an average of 12.1° (measured from the centroid of the Cp* ring), as shown in Figure 6.

Consistent with the solid-state structure, the $^{11}B\{^1H\}$ NMR spectrum of **4** shows four different boron environments at δ 99.0 (1 B), 83.5 (2 B), 46.6 (2 B), and 17.6 (2 B), all of which appear as doublets in the ^1H coupled spectrum. Like **3**, there is a wide spread of chemical shifts, albeit a span of 81 rather than 117 ppm. There are three four-connected vertexes, B(1), B(2,3), and B(6,7), and one five-connected, B(4,5). Thus, B(1) and B(2,3) resonate at low frequency, while B(6,7) appears at high frequency. Although B(4,5) is a four-connected vertex, it is assigned to the resonance at δ 46.6, the bridging hydrogen having the effect of shifting the resonances upfield as observed previously in metallaborane species.[49] Corroboration of this assignment comes from an inspection of the ^{11}B resonances for quasi-isostructural $(Cp^*Re)_2B_7H_7$, **5** (see below), which does not have μ_3-H groups and shows all three four-connected vertexes (assigned by $^{11}B-^{11}B$ COSY NMR) in a similar region at low field (Figure 7).

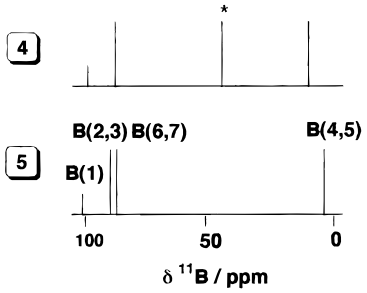

Figure 7. Stick diagram for the ^{11}B resonances in **4** and **5**. The resonance marked with an asterisk is assigned to B(6,7) in **4**.

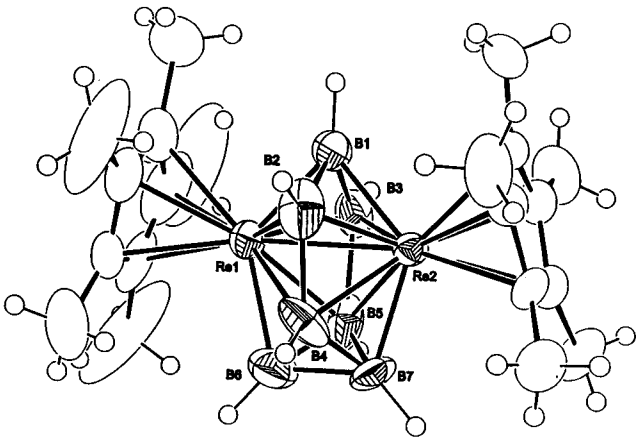

Figure 8. Molecular structure of $(Cp^*Re)_2B_7H_7$, **5.**

In the ^1H NMR spectrum of **4** four signals due to seven BH_t groups (2:1:2:2) and two equivalent Cp* groups are observed, along with an integral 2 H signal at δ −8.9, assigned to the two, equivalent μ_3-H atoms. The latter signal is broader than that in **3** (90 vs 5 Hz), evidencing coupling to boron. The ^1H NMR spectrum of **4** is invariant down to a temperature of −80 °C.

$(Cp^*Re)_2B_7H_7$, 5. In the course of examining the reactivity of Cp^*ReCl_4 with monoboranes we isolated the rhenaborane, $(Cp^*Re)_2B_7H_7$, **5**, in good yield as a pale yellow solid. This compound is isoelectronic with **4**, and its solid-state structure is shown in Figure 8, while salient bond lengths and angles are given in Table 4. The core structures of **4** and **5** are the same. The only gross structural difference (apart from differences in M−B bond lengths between the Re and W) is the absence of μ_3-H groups on **5** and the tilt of the Cp* ligands (Figure 6). The structural consequence of this is that the molecule has overall, approximate, C_{2v} symmetry, the Cp* groups now essentially lying perpendicular to the B(1)−W(1)−B(6)−B(7)−W(2) least-squares plane (1.1° average tilt). The Re−Re bond length at 2.7875(6) Å falls in the range observed for Re−Re single bonds.[50]

As already pointed out above, the $^{11}B\{^1H\}$ NMR spectrum of **5** is similar to that of **4** and has been unambiguously assigned by $^{11}B-^{11}B$ COSY spectroscopy. Consistent with the absence of a μ_3-H group, the four-connected vertex, B(6,7), observed at δ 46.6 in **4** now resonates at lower field, δ 82.1, in the same region as the other four-connected vertexes (B(1) and B(2,3),

(49) Rath, N. P.; Fehlner, T. P. *J. Am. Chem. Soc.* **1988**, *110*, 5345.

(50) Poli, R.; Wilkinson, G.; Moetevailli, M.; Hursthouse, M. B. *J. Chem. Soc., Dalton Trans.* **1985**, 931.

Table 4. Selected Bond Distances (Å) and Bond Angles (deg) for 5

Re(1)−B(1)	2.053(13)	B(1)−B(2)	1.81(2)
Re(1)−B(7)	2.116(14)	B(1)−H(1)	1.1000
Re(1)−B(3)	2.12(2)	B(2)−B(4)	1.80(2)
Re(1)−B(2)	2.14(2)	B(2)−H(2)	1.1000
Re(1)−B(4)	2.231(14)	B(3)−B(5)	1.85(3)
Re(1)−B(5)	2.28(2)	B(3)−H(3)	1.1000
Re(1)−Re(2)	2.7875(6)	B(4)−B(7)	1.73(3)
Re(2)−B(1)	2.062(14)	B(4)−B(6)	1.75(2)
Re(2)−B(3)	2.10(2)	B(4)−H(4)	1.1000
Re(2)−B(2)	2.14(2)	B(5)−B(7)	1.67(3)
Re(2)−B(6)	2.15(2)	B(5)−B(6)	1.69(3)
Re(2)−B(5)	2.271(13)	B(5)−H(5)	1.1000
Re(2)−B(4)	2.28(2)	B(6)−B(7)	1.70(2)
B(1)−B(3)	1.80(2)	B(6)−H(6)	1.1000
		B(7)−H(7)	1.1000
B(1)−Re(1)−B(7)	122.9(5)	B(3)−Re(1)−B(5)	49.7(8)
B(1)−Re(1)−B(3)	51.1(7)	B(2)−Re(1)−B(5)	97.7(6)
B(7)−Re(1)−B(3)	93.9(6)	B(4)−Re(1)−B(5)	67.6(7)
B(1)−Re(1)−B(2)	51.0(7)	B(1)−Re(1)−Re(2)	47.5(4)
B(7)−Re(1)−B(2)	95.0(7)	B(7)−Re(1)−Re(2)	75.4(4)
B(3)−Re(1)−B(2)	90.6(6)	B(3)−Re(1)−Re(2)	48.4(4)
B(1)−Re(1)−B(4)	89.7(7)	B(2)−Re(1)−Re(2)	49.5(4)
B(7)−Re(1)−B(4)	46.8(8)	B(4)−Re(1)−Re(2)	52.7(4)
B(3)−Re(1)−B(4)	97.9(6)	B(5)−Re(1)−Re(2)	52.1(3)
B(2)−Re(1)−B(4)	48.5(7)	B(1)−Re(2)−B(3)	51.3(7)
B(1)−Re(1)−B(5)	90.6(6)	B(1)−Re(2)−B(2)	50.8(7)
B(7)−Re(1)−B(5)	44.5(8)		
B(3)−Re(2)−B(2)	91.1(6)	B(5)−B(3)−Re(1)	69.5(6)
B(1)−Re(2)−B(6)	122.4(6)	Re(2)−B(3)−Re(1)	82.6(6)
B(3)−Re(2)−B(6)	94.7(7)	B(7)−B(4)−B(6)	58.6(10)
B(2)−Re(2)−B(6)	94.1(7)	B(7)−B(4)−B(2)	125.7(10)
B(1)−Re(2)−B(5)	90.6(8)	B(6)−B(4)−B(2)	124.7(11)
B(3)−Re(2)−B(5)	50.0(9)	B(7)−B(4)−Re(1)	63.1(7)
B(2)−Re(2)−B(5)	97.9(6)	B(6)−B(4)−Re(1)	99.4(10)
B(6)−Re(2)−B(5)	44.9(9)	B(2)−B(4)−Re(1)	63.2(7)
B(1)−Re(2)−B(4)	88.1(5)	B(7)−B(4)−Re(2)	97.8(8)
B(3)−Re(2)−B(4)	97.0(6)	B(6)−B(4)−Re(2)	62.9(7)
B(2)−Re(2)−B(4)	47.8(6)	B(2)−B(4)−Re(2)	62.1(7)
B(6)−Re(2)−B(4)	46.4(7)	Re(1)−B(4)−Re(2)	76.3(4)
B(5)−Re(2)−B(4)	66.9(7)	B(7)−B(5)−B(6)	60.9(13)
B(1)−Re(2)−Re(1)	47.2(4)	B(7)−B(5)−B(3)	123.1(11)
B(3)−Re(2)−Re(1)	49.1(4)	B(6)−B(5)−B(3)	123.6(10)
B(2)−Re(2)−Re(1)	49.4(4)	B(7)−B(5)−Re(2)	100.2(9)
B(6)−Re(2)−Re(1)	75.2(5)	B(6)−B(5)−Re(2)	63.8(7)
B(5)−Re(2)−Re(1)	52.3(4)	B(3)−B(5)−Re(2)	60.2(7)
B(4)−Re(2)−Re(1)	51.0(4)	B(7)−B(5)−Re(1)	62.6(6)
B(3)−B(1)−B(2)	114.3(11)	B(6)−B(5)−Re(1)	99.4(9)
B(3)−B(1)−Re(1)	66.5(7)	B(3)−B(5)−Re(1)	60.8(8)
B(2)−B(1)−Re(1)	67.1(7)	Re(2)−B(5)−Re(1)	75.6(4)
B(3)−B(1)−Re(2)	65.5(7)	B(5)−B(6)−B(7)	58.8(10)
B(2)−B(1)−Re(2)	66.9(7)	B(5)−B(6)−B(4)	93.5(11)
Re(1)−B(1)−Re(2)	85.3(5)	B(7)−B(6)−B(4)	60.1(10)
B(4)−B(2)−B(1)	114.2(10)	B(5)−B(6)−Re(2)	71.2(9)
B(4)−B(2)−Re(1)	68.4(7)	B(7)−B(6)−Re(2)	103.8(9)
B(1)−B(2)−Re(1)	62.0(7)	B(4)−B(6)−Re(2)	70.7(8)
B(4)−B(2)−Re(2)	70.1(7)	B(5)−B(7)−B(6)	60.3(11)
B(1)−B(2)−Re(2)	62.2(7)	B(5)−B(7)−B(4)	95.1(9)
Re(1)−B(2)−Re(2)	81.1(5)	B(6)−B(7)−B(4)	61.3(10)
B(1)−B(3)−B(5)	115.0(11)	B(5)−B(7)−Re(1)	72.9(10)
B(1)−B(3)−Re(2)	63.3(7)	B(6)−B(7)−Re(1)	105.6(8)
B(5)−B(3)−Re(2)	69.8(7)	B(4)−B(7)−Re(1)	70.1(6)
B(1)−B(3)−Re(1)	62.4(6)		

Figure 7). The ^{1}H NMR spectrum of **5** shows signals due to two equivalent Cp* groups and a total of seven BH_t groups.

Structure and Bonding of 4 and 5. Given our experience with **3** we were prepared for an unconventional analysis of **4** and **5**, as both compounds have 7 sep and constitute $n - 2$ clusters, 3 pairs short of the normal closo requirement. And, indeed, we were unable to reconcile cluster geometry and electron count using conventional ideas. Our approach was to construct connections between the observed geometry and expected geometries for closo clusters and explore the consequences of the structural perturbations on electronic structure by MO methods.

Two ways of generating the observed structure are shown in Figure 9. In the first (a) we begin with a nine-vertex tricapped trigonal prism. A square pyramidal fragment consisting of capping atom and the four adjacent atoms constituting a rectangular face of the prism is rotated around an axis perpendicular to the face and passing through the capping atom. In doing so, four five-coordinate vertexes are converted into two six- and two four-connected vertexes. The metal fragments are placed in the six-coordinate vertexes, and BH fragments occupy the remaining seven vertexes. Drawing a cross-cage M−M bond generates the observed frameworks of **4** and **5**. Alternatively, one can begin with a dodecahedral, eight-vertex closed structure, which possesses four four-coordinate and four five-coordinate vertexes, and add a BH fragment between two of the four-coordinate vertexes. This converts two of the five-coordinate vertexes to six and adds a four-coordinate vertex. Again, the addition of a cross-cage M−M bond completes the structure.

The connection of **4** and **5** with the tricapped trigonal prismatic geometry indicated in Figure 9 was further explored by carrying out Fenske−Hall MO calculations on **5** in its observed geometry and that of a hypothetical, but reasonable, tricapped trigonal prismatic shape. The calculations based on the observed structure of **5** give a significant HOMO−LUMO gap (6.0 eV), indicating that 7 sep is right for this molecule in the shape it adopts in nature. In addition, MOs corresponding to Re−Re bonding (filled) and Re−Re antibonding (unfilled) interactions are present and the Re−Re overlap population is 0.12, consistent with a single bond. At this level it appears to be a perfectly normal cluster. The question is why?

The calculations on the hypothetical tricapped trigonal prismatic shape exhibit two low-lying unfilled orbitals, suggesting that only the tetraanion (9 sep) would have a respectable HOMO−LUMO gap. A correlation diagram, Figure 10, shows that the framework distortion leading to the observed structure destabilizes a pair of orbitals sufficiently such that they are unoccupied. Note that the C_3 symmetry element of a tricapped trigonal prismatic cluster permits variation in the prescribed sep from 9 to 11.[5] If the asymmetry caused by the presence of the two Re fragments, which is required in order to keep distances reasonable, removes this option, then 10 sep are required. By insisting on a Re−Re cross-cage bond we get back to a 9 sep requirement. In any case it is clear that the shape exhibited by **5** accommodates the 7 sep electron count, and **4** and **5** can be considered examples of ($n - 2$) sep closed clusters.

Conclusions

The classic borane cluster types designated arachno ($n + 3$, sep), nido ($n + 2$, sep), and closo ($n + 1$, sep) must now be considered to be an incomplete set. In addition to hypocloso (n, sep) investigated by others,[40−42]

(51) *Inorganometallic Chemistry*; Fehlner, T. P., Ed.; Plenum: New York, 1992.

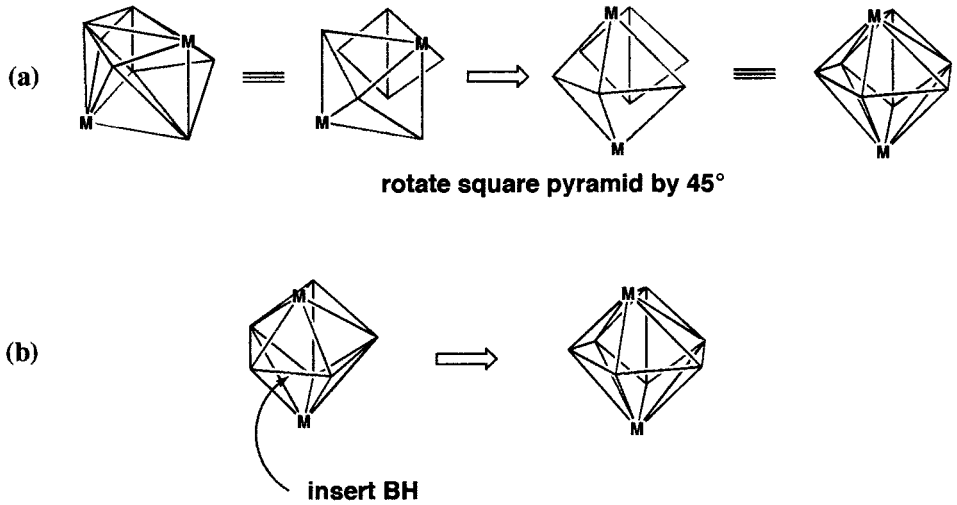

Figure 9. Schematic generation of the cluster framework of **4** and **5** from (a) a tricapped trigonal prism and (b) a dodecahedron.

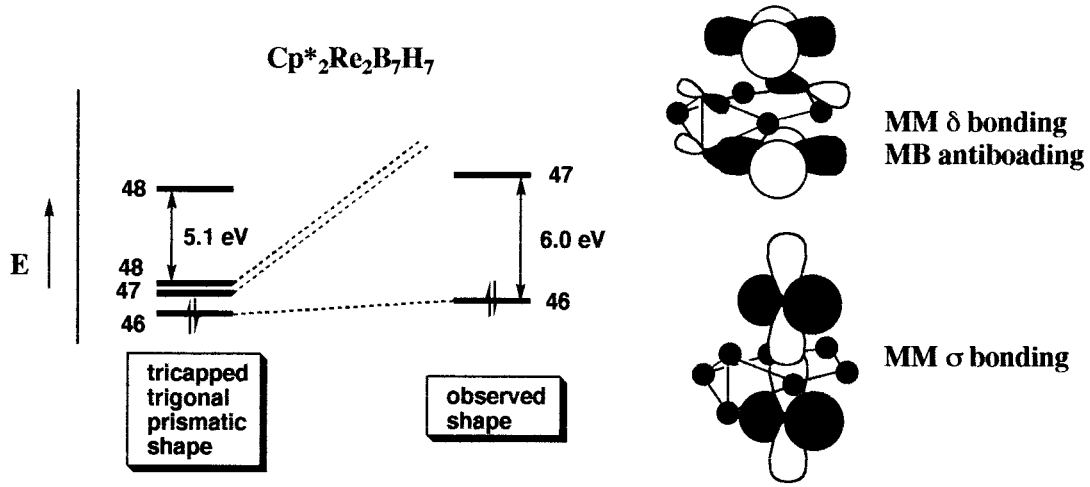

Figure 10. Simplified Fenske−Hall MO correlation diagram for **5** connecting a hypothetical distorted tricapped trigonal prismatic shape and the experimentally determined shape.

we have now provided definitive examples of condensed clusters with ($n - 1$), ($n - 2$), and ($n - 4$) sep. Although such low electron counts are well-known for high-nuclearity transition metal clusters, this is the first time they have been established for metallaboranes and ones predominantly composed of boron. This is surprising, as boron favors cage structures, e.g., the linked cages of elemental boron. In the metal systems, an insufficient number of ancillary ligands results in close packing. In our examples, it is the insufficient number of cluster bonding electrons of the metal fragments that forces a highly compact structure, a demonstration of inorganometallic chemistry.[51]

The chemistry described intersects with other, seemingly disparate, areas. Metallocarbohedrenes have been proposed as a new class of stable molecular clusters.[52−54] These compounds consist of early transition metals and carbon atoms, the latter being isoelectronic with {BH} fragments. Thus, if we removed the Cp* ligands, **3**, **4**, and **5** would be isoelectronic with metcars having compositions $(H)W_3C_8$, $(H)_2W_2C_7$, and Re_2C_7, respectively. Metcars have been described as close packed main group−transition metal clusters, and their proposed structures have been of considerable theoretical interest.[55] Indeed a recent experimental/theoretical paper describes two reasonable structures for the composition Ti_3C_8 which bear some similarities to the structure of **3**.[56] Simply because of the scale of the problem of locating the global minimum, the proposed structures are based on C_2 dimers. One wonders if more contiguous structures such as **3** might have comparable energies. In any case, the factors driving close-packing in **3** appear to be the same as those responsible for the close packed "metcar" structures.

The work also has ties to certain solid-state Zintl phases composed of ligand-free cluster anions which often obey the same cluster electron counting rules followed for molecular main group clusters.[57] For bare group 13 cluster systems high net negative charges are

(52) Guo, B. C.; Kerns, K. P.; Castleman, A. W., Jr. *Science* **1992**, *255*, 1411.
(53) Guo, B. C.; Wei, S.; Purnell, J.; Buzza, S.; Castleman, A. W., Jr. *Science* **1992**, *256*, 515.
(54) Cartier, S. F.; May, B. D.; Castleman, A. W., Jr. *J. Phys. Chem.* **1996**, *100*, 8175.
(55) Bénard, M.; Rohmer, M.-M.; Poblet, J.-M.; Bo, C. *J. Phys. Chem.* **1995**, *99*, 16913.
(56) Wang, Z.-T.; Sinn, E.; Grimes, R. N. *Inorg. Chem.* **1985**, *24*, 826.
(57) Corbett, J. D. *Chem. Rev.* **1985**, *85*, 383.

required to meet Wade's rules, and the exigencies of high charges have been shown to lead to structural changes accommodating a reduction in the net charge. These clusters have been called "hypoelectronic"[58,59] and exhibit as many as 3 sep's below the expected value for the closo structure prescribed by the electron counting rules for the set of fragments in the cluster. The situation is totally analogous to what we find with compounds **4** and **5**, although its origin is different.

Acknowledgment. The assistance of Mr. Donald Schifferl with the NMR experiments as well as the generous support of the National Science Foundation are gratefully acknowledged.

OM980814C

(58) Sevov, S. C.; Corbett, J. D. *Inorg. Chem.* **1991**, *30*, 4875.
(59) Corbett, J. D. *Struct. Bonding* **1997**, *87*, 157.